Wetting between structured surfaces:
Liquid bridges and induced forces

P. S. Swain and R. Lipowsky

Max-Planck Institut für Kolloid- und Grenzflächenforschung - 14424 Potsdam, Germany

Abstract. – Wetting phenomena are theoretically studied for a slab geometry consisting of a wetting phase confined between two chemically patterned substrates. Each of these is decorated by an array of stripes whose composition alternates between two different surface phases. For a single pair of opposing stripes, the wetting phase may either form a bridge spanning from one surface to the other or it may break up into two separate channels. The bridge state induces an effective interaction between the two substrates. This leads to the bridge itself having a preferred contact angle and the substrates having a preferred separation. In the case of many stripes, one has a whole sequence of morphological transitions with the number of bridges decreasing as the surface separation grows.

Consider a liquid, say β, at or close to two-phase coexistence with another fluid phase α, and which is located within a slab between two solid substrates. If both of these have homogeneous surfaces, they may, depending on their chemical nature, be either wetted or dewetted by β. Let us assume that the substrates contain two types of surface domain, denoted by γ and δ, which attract and repel the β-phase, respectively. In such a situation, the β liquid will try to maximise its contact with the γ domains on *both* surfaces, while trying to avoid the δ regions. In this way, the morphology of the intervening wetting structure will reflect the underlying chemical patterning of the two substrates.

From a theoretical point of view, the wetting of structured substrates exhibits several unusual features which have been recently brought to light through studies of *single* surfaces [1–3]. One important new finding is that these systems can undergo morphological transitions in which the wetting phase experiences an abrupt change in shape.

In this letter, we will study the possible wetting morphologies within a structured slab. We will focus on the simplest type of substrate pattern, consisting of alternating γ- and δ-stripes. These are of width L_γ, length $L_{\gamma\delta}$ and lie parallel to but not necessarily exactly opposite a stripe on the other surface. Any mismatch is described by $L_\parallel$ (see fig. 1). A similar geometry, though with sinusoidally structured substrates, has been recently studied by Monte Carlo simulations [4] and by density functional theory [5].

We will concentrate on wetting structures which are, at least, of the size of microns and so ignore line tension. Furthermore, the roughness of the $\alpha\beta$ interfaces is always small and
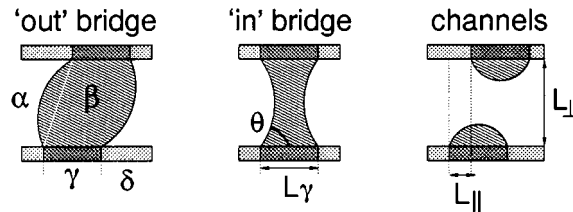
Fig. 1 – Different β-phase morphologies within a structured slab. Dark γ patches on the substrate attract β while light δ regions are repulsive. For $\Delta p < 0$, either a bridge state that bulges outwards or the two-channel state exists. For $\Delta p > 0$, M changes sign and the bridge curves inwards.

comparable to the size of the molecules. Thus, it is sufficient to adopt a mean-field approach and consider only arrangements of the β-phase which are minima of the free energy. Defining Σ as the interfacial free energy of the $\alpha\beta$ interface, the latter is

$$\mathcal{F} = \Sigma A_{\alpha\beta} - (\Sigma_{w\alpha} - \Sigma_{w\beta})A_{w\beta} + \Delta p\, V\,. \tag{1}$$

Here, $\Sigma_{w\alpha}$ and $\Sigma_{w\beta}$ are the interfacial free energies between the wall and the α and β phases, respectively. Due to the chemical heterogeneity of the surface these will be a function of position. There is a volume V of β which interfaces with a contact area $A_{w\beta}$ to the substrate surface and with an area $A_{\alpha\beta}$ to the α phase. Finally, we need to choose an appropriate ensemble to work in. One can fix the pressure difference, defined as $\Delta p = p_\alpha - p_\beta$, across all $\alpha\beta$ interfaces. This then leads to a term in (1) representing the work done against Δp to create V of β. It is a genuine contribution to the free energy. Alternatively, one can opt for a fixed volume ensemble, in which the total volume of β in the system is confined to V. In this case, the $\Delta p\, V$ term still appears but does so only to enforce the volume constraint. The parameter Δp is a Lagrange multiplier and should be ignored in any calculations of the free energy.

Minimising (1) with respect to the shape of the β-surface leads to the Laplace equation, $\Delta p = -2\Sigma M$, where M is the mean curvature of the $\alpha\beta$ interface. Further minimisation with respect to the configuration of the three phase (α-β-substrate) contact line, gives the generalised Young equation [2,6]

$$\Sigma_{w\alpha}(\boldsymbol{x}) = \Sigma_{w\beta}(\boldsymbol{x}) + \Sigma \cos\left[\theta(\boldsymbol{x})\right] \tag{2}$$

for the contact angle θ. As already mentioned, the chemical patterning results in a contact angle which varies with position. Here, $\boldsymbol{x}$ is a vector in the plane of the surface under consideration. Regarding, for the moment, a single substrate, let θ_δ and θ_γ be the contact angles taken up on the more lyophobic (α favouring) and more lyophilic (β favouring) regions, respectively. Then, the contact angle of the β-phase will continually shift between these two values as its contact line crosses each chemically distinct area. Moving from a γ to a δ patch, θ will gradually increase from θ_γ to θ_δ. This change will occur in a narrow border region between the two chemically pure sections. If surfaces are considered for which the width of these border regions are small compared to the linear size of the domains themselves, then the substrate interfacial free energies, $\Sigma_{w\alpha}$ and $\Sigma_{w\beta}$, become almost discontinuous. Equation (2) then implies that at this $\gamma\delta$ divide, the contact angle is not specified but is simply bounded; $\theta_\gamma \leq \theta \leq \theta_\delta$ [2]. If a drop is large enough that it entirely covers the lyophilic region, then the freedom in θ implies that the drop's *shape* will change as one alters either its volume or Δp.

For simplicity, we will take the extreme cases of $\theta_\gamma = 0$ and $\theta_\delta = \pi$, *i.e.* complete wetting and complete dewetting of the γ- and δ-domains, respectively. This means that, providing V

is of a certain size, the lyophilic areas will nearly always be covered and the lyophobic domains nearly always left clear. The contact line is "pinned" to the $\gamma\delta$ border.

Before proceeding, we remark that our system is effectively two-dimensional since we consider very long stripes with $L_{\gamma\delta} \gg L_\gamma$ and ignore the possibility of symmetry breaking configurations (see [3] for a counterexample). Thus, each bridge will have a constant cross-section whose contour we need only determine. The Laplace equation implies that all β-phase surfaces will be of fixed mean curvature, $M = -\Delta p/2\Sigma$, and so that the contour line will be a segment from a circle whose radius, R, obeys

$$R = \Sigma/|\Delta p| \,. \tag{3}$$

The different possible configurations are shown in fig. 1. When $L_\perp$ becomes large enough a β-bridge is no longer stable and breaks into two β-channels (again these have constant cross-section and each cover an entire lyophilic stripe). In addition to this broken state, one can have a bridge bulging outwards ($\Delta p < 0$) and one which curves inwards ($\Delta p > 0$). Our remit is to find which of these morphologies are stable as one changes $L_\perp$ and/or $L_\parallel$.

Considering an isolated pair of stripes (one on each substrate), elementary geometry implies that the reduced volumes, $\bar{V} = V/L_{\gamma\delta}$, are given by

$$\bar{V}_{\mathrm{ch}} = 2R^2 \Psi(L_\gamma/2R) \tag{4}$$

for the channel state, with contact angle $\theta \le \pi/2$ and $\Psi(x) = \arcsin x - x\sqrt{1-x^2}$; while

$$\bar{V}_{\substack{\mathrm{in}\\\mathrm{out}}} = L_\gamma L_\perp \mp 2R^2 \Psi\left(\sqrt{L_\perp^2 + L_\parallel^2}/2R\right) \tag{5}$$

for the bridge. Here "in" and "out" refer to bridges with Δp positive and negative, respectively.

In order to calculate the free energies of these possible shapes (and so find the most stable one), the ensemble needs to be specified. Using (1) with $w = \gamma$, and remembering that $\Sigma_{\gamma\alpha} - \Sigma_{\gamma\beta} = \Sigma \cos\theta_\gamma = \Sigma$ since $\theta_\gamma = 0$, we find for the reduced free energies, $\bar{\mathcal{F}} = \mathcal{F}/(\Sigma_{\alpha\beta}L_{\gamma\delta})$, the simple expressions

$$\bar{\mathcal{F}}_{\mathrm{ch}} = 4R\arcsin(L_\gamma/2R) - 2L_\gamma \quad \text{and} \quad \bar{\mathcal{F}}_{\mathrm{br}} = 4R\arcsin\left(\sqrt{L_\perp^2 + L_\parallel^2}/2R\right) - 2L_\gamma \tag{6}$$

in the constant-volume ensemble. For the constant-pressure case, the $\Delta p \bar{V}$ term in (1), specified by (3) and (4), (5), should be added.

The fixed-pressure ensemble has the simplest morphology diagram. For $\Delta p < 0$, we can only have bridges which bulge outwards. These become unstable when their free energy is equal to that of the two-channel state and the corresponding transition line is given by

$$4R^2 \arcsin\left(\sqrt{L_\perp^2 + L_\parallel^2}/2R\right) - \bar{V}_{\mathrm{out}}(R) = 4R^2 \arcsin(L_\gamma/2R) - \bar{V}_{\mathrm{ch}}(R) \,. \tag{7}$$

Equation (3) defines R in terms of Δp, and (7) describes an arc dividing the upper right-hand quadrant of the $L_\parallel L_\perp$ plane. For low $L_\perp$, one has a bridge; while for high, always the channel state. For $\Delta p > 0$, the change in the sign of M implies that the "in"-bridge can only coexist with a thin-film state, whose shape is governed by the interplay between the pressure and intermolecular forces. Since we can ignore these forces on the mesoscopic scales considered here, the film is characterised by $V = 0$ and $A_{\alpha\beta} = A_{\beta\gamma}$. Hence from (1), it has zero free energy, and the transition line is then given by $\bar{\mathcal{F}}_{\mathrm{br}} + \bar{V}_{\mathrm{in}}/R = 0$. As Δp becomes small, both transition lines tend to the circle given by $L_\perp^2 + L_\parallel^2 \approx L_\gamma^2$.
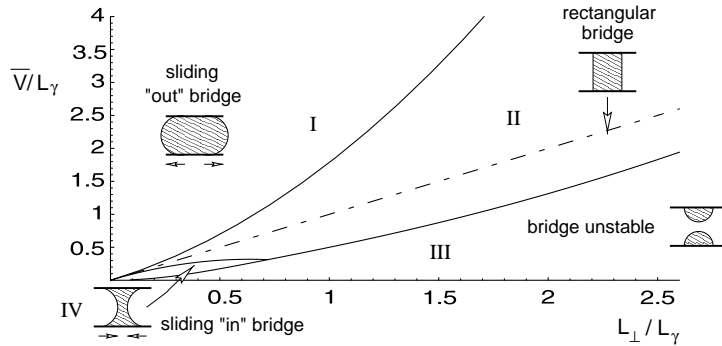
Fig. 2 – Morphology diagram for a single pair of γ-stripes of width L_γ and with $L_\parallel = 0$. Four different regions are present, see text. The arrows on the sketches of the sliding bridges indicate the direction of slide as the volume is increased/decreased for the "out"/"in" cases.

The constant-volume ensemble, however, is more interesting and we will concentrate on it for the remainder of the paper. Given a fixed volume of β-phase, R can be calculated by setting the right-hand side of (4) or (5) equal to that volume. One needs then only to compare (6) to find the most likely state. The result is shown in fig. 2 for the simple case when $L_\parallel = 0$. There exist four main morphologies that have their own regions of stability. In area I, a "sliding" bridge is the stable configuration. The value of $L_\perp$ is so small and the volume of β so large that the bridge bulges outwards as much as possible and attains a contact angle of $\theta = \theta_\delta = \pi$. Consequently, for large volumes the $\alpha\beta$ interface is forced to move onto the δ region. We refer to this state as a "sliding" bridge as each of its surfaces, which are perfect half circles, will drift across the δ region either towards or away from the γ stripe, as the volume shrinks or grows, respectively. At the morphology boundary, the bridge surfaces follow the $\gamma\delta$ divide, and in region II, where the bridge is still stable, they remain pinned there. The dashed line in fig. 2 marks where a bridge changes from an "out" to an "in" configuration as $L_\perp$ increases. The bridge breaks in region III and the two-channel state has the lowest free energy. Finally, IV indicates a region where the contact angle of the bridge has been reduced to $\theta = \theta_\gamma = 0$ and so, for low volumes, the bridge retreats back on the lyophilic stripe. For
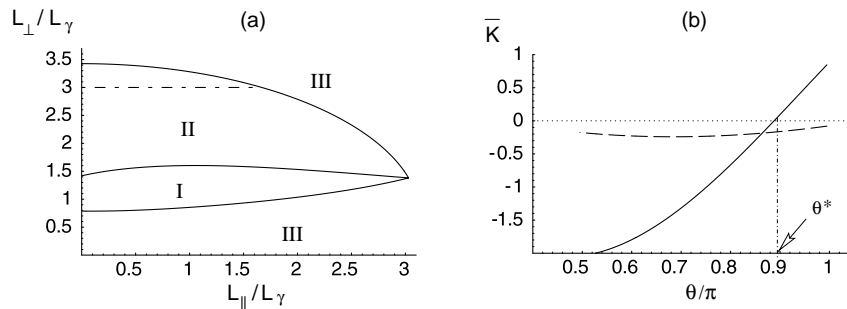

Fig. 3 – The morphology and force diagrams for a system with a fixed volume, $\bar{V} = 3L_\gamma^2$. On the dash-dotted line in (a) the bridge is rectangular. (b) shows $\bar{K}_\parallel < 0$ (dashed curve) and $\bar{K}_\perp$ (heavy line), which changes sign at $\theta = \theta^*$. The value of θ is increased by decreasing $L_\perp$ and the curves are limited by the bridge becoming unstable (low θ) or touching the δ regions (high θ).

real systems, the sliding bridges of I and IV may well be replaced by states which are not translationally invariant along the stripes and so no longer have a constant cross-section. An example for $L_\parallel \neq 0$ is shown in fig. 3a, with the different regimes having the same definitions as above.

The existence of a β-bridge spanning the two substrates implies that an attempt to move either of them will experience a force as the shape of the bridge changes. We shall consider only the force generated in response to shifting the substrates in directions normal, $\bar{K}_\perp$, and parallel, $\bar{K}_\parallel$, to their surfaces. These are defined as $\bar{K}_\perp \equiv -\partial\bar{\mathcal{F}}_{\rm br}/\partial L_\perp$ and $\bar{K}_\parallel \equiv -\partial\bar{\mathcal{F}}_{\rm br}/\partial L_\parallel$, and have to be rescaled by $\Sigma L_{\gamma\delta}$ before having the correct dimensions. Working in the fixed-volume ensemble, we find, after some algebra, that the perpendicular force is given by

$$\bar{K}_\perp = 2\Big\{L_\perp \cos(\phi + \theta) - L_\gamma \sin(\phi + \theta)\Big\}\Big/\sqrt{L_\perp^2 + L_\parallel^2} \tag{8}$$

and the parallel force by

$$\bar{K}_\parallel = 2L_\parallel \cos(\phi + \theta)\Big/\sqrt{L_\perp^2 + L_\parallel^2}\,, \tag{9}$$

where $\tan\phi = L_\perp/L_\parallel$ and θ is defined to be the contact angle in the bottom left-hand corner of the bridge, see fig. 1. Using (5), one can calculate R for a fixed $\bar{V}$, which is then simply related to θ via $\sin(\phi + \theta) = \mp\sqrt{L_\perp^2 + L_\parallel^2}/2R$, for "out"- and "in"-bridges, respectively. It is worth remarking that $\bar{K}_\parallel$ is always negative (it can be shown that $\pi/2 \leq \phi + \theta \leq 3\pi/2$) and so there is always resistance to shearing the substrates. However, there exists a characteristic contact angle θ^* for which $\bar{K}_\perp$ changes sign. From (8),

$$\tan(\phi + \theta^*) = L_\perp/L_\gamma \tag{10}$$

which becomes $\tan\theta^* = -L_\gamma/L_\perp$ for $L_\parallel = 0$. Note that $\pi - \phi < \theta^* < 3\pi/2 - \phi$ and so $\bar{K}_\perp$ only vanishes when $\Delta p < 0$, *i.e.* for an "out" bridge. One can show that the free energy has a minimum as a function of θ at $\theta = \theta^*$. Thus, $\bar{K}_\perp$ always acts to bring the system into a configuration for which the bridge contact angle is θ^*. The typical behaviour of the forces, as a function of θ, is shown in fig. 3b.

Finally, we consider scenarios where the substrates are decorated with identical periodic arrays of stripes. Let the number of pairs of stripes and the number of bridges present be $N_{\rm st}$ and $N_{\rm br}$, respectively. For the pressure ensemble, each pair of stripes will act independently and the corresponding phase diagram will be identical to that described above for a single pair. However, in the volume ensemble, where, after any small perturbation, the β-phase is allowed to re-distribute to its most stable configuration, the situation is quite different. The material transport, which is expected to be relatively slow if α is a vapour phase but quite fast if it is another liquid, implies a cooperative behaviour between the different morphologies.

In addition to the bridges, channels and thin films already discussed, one should also include a layered state, with flat layers of β-phase on each surface covering both lyophobic and lyophilic regions. To calculate its free energy, $\bar{\mathcal{F}}_{\rm la}$, we need to specify the width of the δ-stripes; let this be L_δ. Using (1) and remembering that $\theta_\gamma = 0$ and $\theta_\delta = \pi$, we find $\bar{\mathcal{F}}_{\rm la} = 4N_{\rm st}L_\delta$. For a given system, the stable state can then be found by comparing the free energies of all possible combinations of the different morphologies.

In fig. 4a we show $N_{\rm br}$ for 100 pairs of stripes (sliding is not included) as $L_\perp$ is varied. The system has to have a certain size before it can accommodate all the β-phase, but then the large volume forces it to exist in the layered state ($N_{\rm st} \equiv -1$). As soon as bridges can exist, they cover all the γ-stripes. This is then followed by a gradual cascade in their number. From (6), the free energy, as a function of the mean curvature M, is only properly defined
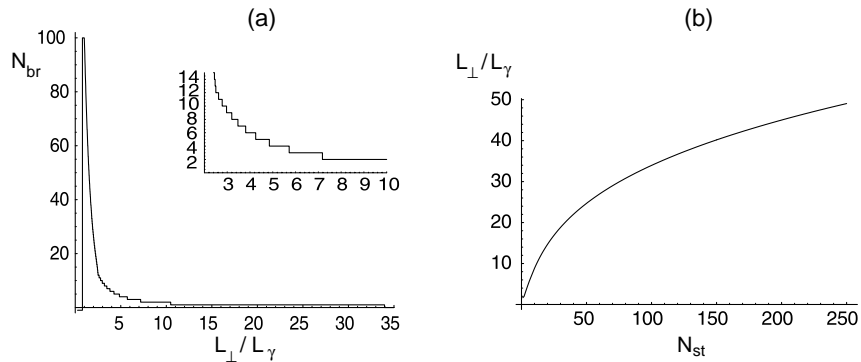
Fig. 4 – Structured slab with many γ stripes, $L_{\parallel} = 0$ and $L_\delta = 3L_\gamma$. The (reduced) volume of the β-phase in each case is $N_{\mathrm{st}}L_\gamma^2$. In (a), a system with $N_{\mathrm{st}} = 100$ is shown. The stable number of bridges gradually reduces as $L_\perp$ is increased. The inset is an enlargement of part of the curve. (b) gives the maximum value of $L_\perp$ for which a bridge can exist as a function of the number of stripes.

for $0 \leq M \leq \min(L_\gamma^{-1}, L_\perp^{-1})$. For $N_{\mathrm{st}} \gg 1$, it transpires that if $L_\perp > L_\perp^{(1)}(\bar{V}/N_{\mathrm{st}})$, the total free energy no longer has a true minimum but is optimised by an endpoint value of M, *i.e.* $M = L_\perp^{-1}$. For example, when $\bar{V}/N_{\mathrm{st}} = L_\gamma^2$, one has $L_\perp^{(1)} \simeq 1.91L_\gamma$. The volume constraint then gives that

$$N_{\mathrm{br}} = (\bar{V} - N_{\mathrm{st}}\bar{V}_{\mathrm{ch}})/(\bar{V}_{\mathrm{br}} - \bar{V}_{\mathrm{ch}})\big|_{R=L_\perp/2} \,, \tag{11}$$

which represents an implicit equation for those $L_\perp$ at which N_{br} undergoes an abrupt change. Equation (11) implies $N_{\mathrm{br}} \sim L_\perp^{-2}$ for large $L_\perp$. For $L_\perp > L_\perp^{(1)}$, the contact angle $\theta = \pi$ and consequently sliding effects can become important. Indeed, there exist two regimes, where bridges detached from the lyophilic stripes are the most stable states. For $L_\perp < L_\perp^{(0)} \equiv 2L_\gamma \left[\sqrt{1 + \pi\bar{V}/(N_{\mathrm{st}}L_\gamma^2)} - 1\right]/\pi$, the system prefers to exists as N_{st} bridges, all of which have swollen so much that they have slid off their original γ-stripe, rather than being in the layered state. Similarly, for large $L_\perp > L_\perp^{(2)} \equiv \lambda^{-1}L_\gamma$, a single sliding bridge is the equilibrium morphology. Here, $\lambda^{-1} \simeq 2.51$ and obeys $\lambda(2 + \sqrt{1 - \lambda^2}) = \arccos\lambda$. As $L_\perp$ is increased further, the width of this bridge gradually decreases as it moves inwards. Eventually, it reattaches and its curvature falls below $L_\perp^{-1}$. So far, we have implicitly assumed that $L_\delta \gg L_\gamma$. If this is not true the situation becomes even more complicated as the detached bridges will cover more than one lyophilic region. However, in real systems, we would expect the sliding states to be precursors to morphologies which break both the x_1 and x_2 symmetries. Such "modified" drops have already been observed experimentally [7].

In fig. 4b, we plot, for a system with a given N_{st}, the highest value of $L_\perp$ for which a bridge can exist. This has direct experimental relevance as it is the maximum $L_\perp$ for which a force acts between the two substrates.

In summary, we have investigated wetting phenomena occurring between two, flat, parallel, lyophobic substrates each of which is structured by lyophilic stripes. We have shown that a number of different morphologies of the wetting phase are possible. In particular, a bridge can span from a lyophilic stripe on one surface to another on the opposite surface and so cause a force to act between the substrates. This can be attractive or repulsive and vanishes at a special contact angle of the bridge, θ^*. Our model also predicts regimes where the bridge detaches from the stripes, which could well be precursors for transitions to broken-

symmetry states. When many stripes are considered, we can find analytically the number of stable bridges as the substrates are pulled apart. Experimentally, a slab geometry can be realised by, for example, the two opposing surfaces of a surface force apparatus. Similarly, an atomic force microscope consists of a highly curved surface, the "tip", which is brought into contact with another, less curved, surface. These surfaces can be structured using the many preparation methods which are now available. These include elastomer stamps [8,9] vapour deposition through grids [7,10], photolithography of amphiphilic monolayers [11], lithography with colloid monolayers [12], atomic beams modulated by light masks [13] and microphase separation in diblock copolymer films [14]. Recent observations of water bridges which can form between the tip of an atomic force microscope and the surface which it is patterning [15], have given new relevance to our work and, in a following publication, we will extend the results to include substrates decorated with circular lyophilic domains.

REFERENCES

[1] Lipowsky R., Lenz P. and Swain P. S., to be published in *Colloid Surf. A*.
[2] Lenz P. and Lipowsky R., *Phys. Rev. Lett.*, **80** (1998) 1920.
[3] Gau H., Herminghaus S., Lenz P. and Lipowsky R., *Science*, **283** (1999) 46.
[4] Schön M. and Diestler D. J., *Chem. Phys. Lett.*, **270** (1997) 339.
[5] Röcken P., Somoza A., Tarazona P. and Findenegg G., *J. Chem. Phys.*, **108** (1998) 8689.
[6] Swain P. S. and Lipowsky R., *Langmuir*, **14** (1998) 6772; Wolansky G. and Marmur A., *Langmuir*, **14** (1998) 5292.
[7] Mönch W., *Dynamik von Flüssigkeiten auf strukturierten Substraten*, doctoral thesis, Universität Konstanz (1999).
[8] Drelich J., Miller J. D., Kumar A. and Whitesides G. M., *Colloid Surf. A*, **93** (1994) 1.
[9] Morhard F., Schumacher J., Lenenbach A., Wilhelm T., Dahint R., Grunze M. and Everhart D. S., *Electrochem. Soc. Proc.*, **97** (1997) 1058.
[10] Herminghaus S., Fery A., and Reim D., *Ultramicroscopy*, **69** (1997) 211.
[11] Möller G., Harke M., Motschmann H. and Prescher D., *Langmuir*, **14** (1998) 4955.
[12] Burmeister F., Schafle C., Matthes T., Bohmisch M., Boneberg J. and Leiderer P., *Langmuir*, **13** (1997) 2983.
[13] Drodofsky U., Stuhler J., Schulze T., Drewsen M., Brezger B., Pfau T. and Mlynek J., *Appl. Phys. B*, **65** (1997) 755.
[14] Heier J., Kramer E. J., Walheim S. and Krausch G., *Macromolecules*, **30** (1997) 6610.
[15] García R., Calleja M. and Pérez-Murano F., *Appl. Phys. Lett.*, **72** (1998) 2295.